Research Article

Journal of Environmental Nanotechnology

Photocatalytic Degradation of Transition Metal (Ni)-Doped ZnS Nanoparticles Synthesized *via* Simple Solvothermal Route

K. Valliyammal* and R. Sakthi Sudar Saravanan
Physics Research Centre, Chikkanna Government Arts College, TN, India
Received: 18.07.2024 Accepted: 25.09.2024 Published: 30.09.2024
*nithy.n@gmail.com

ABSTRACT

Ni-doped ZnS nanoparticles were obtained using the simple Solvothermal Microwave Irradiation (SMI) method in this research. This technique is cost-effective and results in a high level of uniformity in particle size. The structural characteristics of the sample were examined using XRD, FESEM imaging, and elemental analysis obtained from the EDX spectrum, while the optical properties were analyzed through UV–Visible absorption studies. The XRD pattern of Ni-doped ZnS nanoparticles was used to determine the crystallite size (D), lattice constant (a), and unit cell volume (V). As the concentration of Ni dopant increased (0, 2.5, 5.0 M %), the values of the lattice constant decreased, leading to an overall decrease in the volume of the unit cell. The FESEM images reveal that the sample has a uniform surface morphology, while EDX analysis confirms the presence of Zn, Ni, and S elements in the sample. The dimensions of Ni-doped ZnS nanoparticles strongly influence their optical properties. The optical bandgap, as obtained from UV-Vis measurements, ranges from 3.54 eV to 3.50 eV with doping concentrations varying from 0 M% to 5.0 M% .This adjustment in optical properties suggests that Ni-doped ZnS nanoparticles have diverse applications in optoelectronics, sensors, UV detectors, and as an efficient photocatalyst for degrading pollutants in water. The efficiency of the degradation of Methylene Blue dye by Ni-doped ZnS nanoparticles was found to be 75.19%.

Keywords: Ni-doping, ZnS nanoparticles; Solvothermal microwave irradiation; Photocatalyst.

1. INTRODUCTION

Nowadays, the search for new materials focuses on multifunctional properties across multiple disciplines. Such materials are expected to address environmental challenges and meet human needs. The scientific community continues to explore novel multifunctional materials to mitigate water and environmental pollution. In this context, Group II–IV compounds have attracted significant interest due to their unique morphological and optical properties (Krishnan *et al*.2019; Rajabi and Farsi, 2015). The wide band gap of non-toxic ZnS nanomaterials (3.0–3.77 eV) is crucial for optoelectronic applications. These materials exhibit important optical, electrical, and photocatalytic properties, making them suitable for the development of solar cells and other optoelectronic devices. Various physical and chemical methods, such as hydrothermal processes (Wu *et al.* 2017), sonochemical (Amiri *et al*. 2014), chemical bath deposition (Zeinand Alghoraibi, 2019), solid state method (Farooqi and Srivastava, 2014), coprecipitation method (Srivastava *et al*. 2013), microwave assisted irradiation method (La *et al.* 2013), solvothermal microwave irradiation (SMI) technique (Gowdhaman *et al.* 2021) etc., were employed to obtained ZnS nanoparticles. The SMI technique is considered one of the most effective ways to produce ZnS nanomaterial because the particles are minimized dimension, have a consistent shape, and the method guarantees safety and high purity (Gowdhaman *et al.* 2021). The customization of nonmaterial properties for device use through the addition of appropriate materials is a well-established practice. When semiconductor nanoparticles are doped with transition elements such as Cd, Ag, Cu, Ni, Co and Mn, new possibilities arise due to entire characteristics change the host material, ZnS (Ramasamy *et al.* 2012).

Through the process of doping, significant enhancements have been made to the fundamental physical characteristics of ZnS, particularly for the purposes of optoelectronic device utilization (Xu *et al.* 2018). The inclusion of Cu in ZnS material enables precise band gap manipulation, expanding its potential for use in high-performance optoelectronic device components such as solar cell windows and in the photocatalytic degradation of industrial dyes showed by (Wang *et al.* 2019). Transition metal (Fe) doped ZnS nanoparticles in photocatalytic activity on Turquoise Blue H5G dye is superior to that of pure ZnS reported by Suganthi and Pushpanathan, (2019). Controlled precipitation method was used to dope Cu (0.1%) with ZnS for studying their characteristic change. Cu (0.1%)

doped ZnS nanoparticles reported optical bandgap value (E_g) changes from 4.41-4.47 eV. The average of particle size of the as synthesized sample was found to be about 2.0–10.0 nm reported by Pouretedal and Keshavarz, (2010).

With these advantageous properties, ZnS nanoparticles are considered promising materials for various electronic applications. In ZnS, Ni dopants act as effective acceptor states that modify the optical properties. When Ni ions substitute Zn lattice sites, they introduce trapping centers for charge carriers, which suppress recombination and thereby enhance photocatalytic efficiency (Kaur *et al*. 2015). Jothibas *et al*. (2018) have used solid state method to prepared doped Ni (0.5-2.0%) with ZnS for tuning the bandgap and the crystallite size also increased with increase dopant. The distance between valance and conduction value (E_g) changed from 3.58 eV to 3.97 eV.

Pure and Ni-doped ZnS nanoparticles (0, 2.5, and 5.0 mol%) were synthesized using a simple solvothermal microwave irradiation (SMI) method. The structural, morphological, and optical properties were comprehensively characterized using XRD, FESEM, EDX, HRTEM, and UV–visible spectroscopy.

2. EXPERIMENTAL METHODS

For pure and different concentration (2.5 M% and 5.0 M %) of Ni-doped ZnS nanoparticles, the reactants $Zn(CH_3COO)_2{\cdot}2H_2O$, $Ni(OCOCH_3)_2{\cdot}4H_2O$, NH_2CSNH_2, and ethylene glycol were purchased from Sigma-Aldrich. The cost-effective simple solvothermal microwave irradiation method (SMI) was used to synthesizing the above nanoparticles (Saravanan *et al*. 2012). In order to synthesise 2.5 M% of Ni-doped ZnS nanoparticles, a solution was prepared by dissolving 0.1M of Zn (II) acetate dihydrate and 0.025 M of nickel(II) acetate tetrahydrate in 50 mL of ethylene glycol. Subsequently, a solution of 0.3 M of thiourea in 50 mL ethylene glycol was introduced gradually into the previously described mixture, with continuous stirring. To get a homogeneous solution, the mixture was agitated vigorously for one hour. A double-walled microwave-safe bowl was employed to contain the resultant homogenous solution. The solution was heated in a domestic microwave oven (Model No. IFB 23BC4 23 L) until a colloidal precipitate was obtained. The resulting colloidal precipitate was cooled to ambient temperature and purified with double-distilled water and acetone to remove any remaining contaminants and unreacted starting materials. The same method was used for the synthesis of 5.0 M% Ni-doped ZnS nanoparticles. To synthesize pure ZnS nanoparticles, a solution was prepared by dissolving 0.1 M of Zn(II) acetate dihydrate in 50 mL of ethylene glycol. A 0.3 M solution of thiourea in 50 mL of ethylene glycol was then added gradually to the aforementioned mixture while maintaining continuous stirring. To achieve a homogeneous solution, the mixture was vigorously agitated for one hour, and the previously described process was employed to obtain pure ZnS nanoparticles.

3. PHOTODEGRADATION OF METHYLENE BLUE (MB) DYE

The synthesized Ni-doped ZnS nanoparticles were evaluated for their photocatalytic activity in degrading methylene blue (MB) dye in aqueous solutions. A stock solution of MB was prepared at a concentration of 10 mg/L, and 30 mg of the as-prepared Ni-doped ZnS nanoparticles were added to 100 mL of this solution. The mixture was stirred using a magnetic stirrer for one hour to ensure uniform dispersion of the nanoparticles and enhance their interaction with the dye molecules. Following this, the combined solution was exposed to ultraviolet (UV) radiation, which excited the electrons in the nanoparticles, generating reactive species capable of degrading the MB dye. Samples were extracted at 30-minute intervals over a total period of 120 minutes and analyzed using a UV-Vis spectrophotometer to measure the absorbance at the dye's characteristic wavelength.

4. RESULTS AND DISCUSSION

4.1 Structural Analysis

Fig. 1 presents the X-ray diffraction (XRD) patterns of Ni-doped ZnS nanoparticles at doping concentrations of 0 M%, 2.5 M%, and 5.0 M%. The analysis reveals that the synthesized nanoparticles exhibit a cubic ZnS structure, consistent with the standard JCPDS Card No. 05-0566, as reported by Tiwary *et al.* (2021) and Patel *et al*. (2018). Importantly, no impurities or secondary phases were observed, confirming the successful incorporation of nickel into the ZnS lattice. The structural integrity of the Ni-doped nanoparticles is attributed to the smaller ionic radius of Ni (0.69 Å) compared to that of the zinc (Zn) atom (0.74 Å), facilitating its substitution without distorting the cubic framework.

As the Ni doping concentration was increased from 2.5 M% to 5.0 M%, notable changes in the XRD peaks were observed, including alterations in intensity and broadening, which suggest variations in crystallite size and potential strain within the nanoparticles. The XRD data were employed to derive key structural parameters such as crystallite size, lattice constant, and unit cell volume. Utilizing Bragg's equation ($n\lambda = 2d \sin\theta$), the interplanar spacing was calculated, while the average crystallite size was estimated through Scherer's formula (Tiwary *et al*.2021; Hussein, 2023).

$$D = K\lambda / \beta\cos\theta \quad \ldots (1),$$

where, K is a dimensionless shape factor it, has a typical value of about 0.9. The Bragg's diffraction angle is represented by 'θ (degree), while the FWHM of diffraction peaks at 2θ (degree) is denoted by β, and λ represents the wavelength (nm) of the X-ray used.

Table 1. The structural parameters of Ni (0, 2.5, and 5.0) M% doped ZnS nanoparticles

Chemical Composition	Crystallite Size(nm)	Inter Planar Spacing 'd' Å	Lattice Constant a (Å)	Volume of a Unit Cell ('a^3' (Å)^3)
Pure ZnS	7.01	3.198	5.384	155.72
2.5% Ni-doped ZnS	6.32	3.634	5.362	153.99
5.0% Ni-doped ZnS	6.09	3.762	5.352	149.72

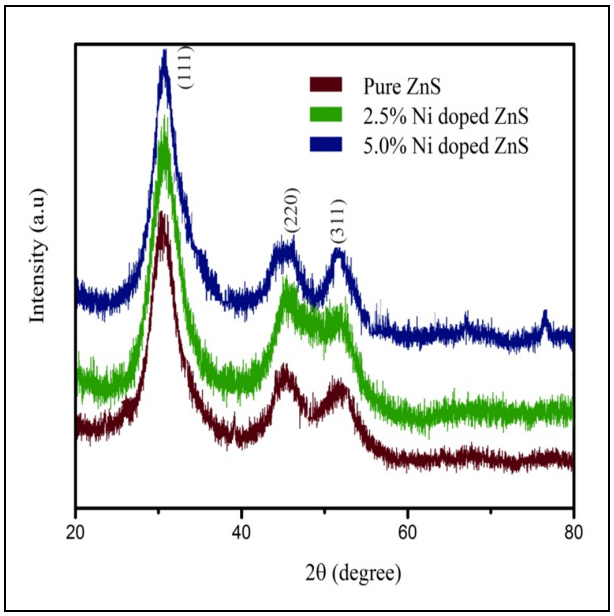


Fig. 1: XRD patterns of Ni (0, 2.5, 5.0) M% doped ZnS nanoparticles

From the obtained structural data, an interesting trend was noted: as the concentration of Ni increased, the lattice constant exhibited a decrease, resulting in a corresponding reduction in the volume of the unit cell. Table 1 summarizes the structural parameters of both pure and Ni-doped ZnS nanoparticles, highlighting the significant effects of doping on their crystallographic characteristics.

The FESEM images (Fig. 2) reveal the structural characteristics of Ni-doped ZnS nanoparticles at doping concentrations of 0 M%, 2.5 M%, and 5.0 M%. Notably, the analysis indicates that while pure ZnS nanoparticles exhibit larger particle sizes, the introduction of nickel as a dopant leads to a reduction in particle size. This size modification can be attributed to the incorporation of Ni ions into the ZnS lattice, which influences the nucleation and growth processes during synthesis. The observed agglomeration of nanoparticles is consistent with findings by Chen *et al.* (2013) and suggests that the dopant may enhance the stability of smaller particle sizes through altered interparticle interactions.

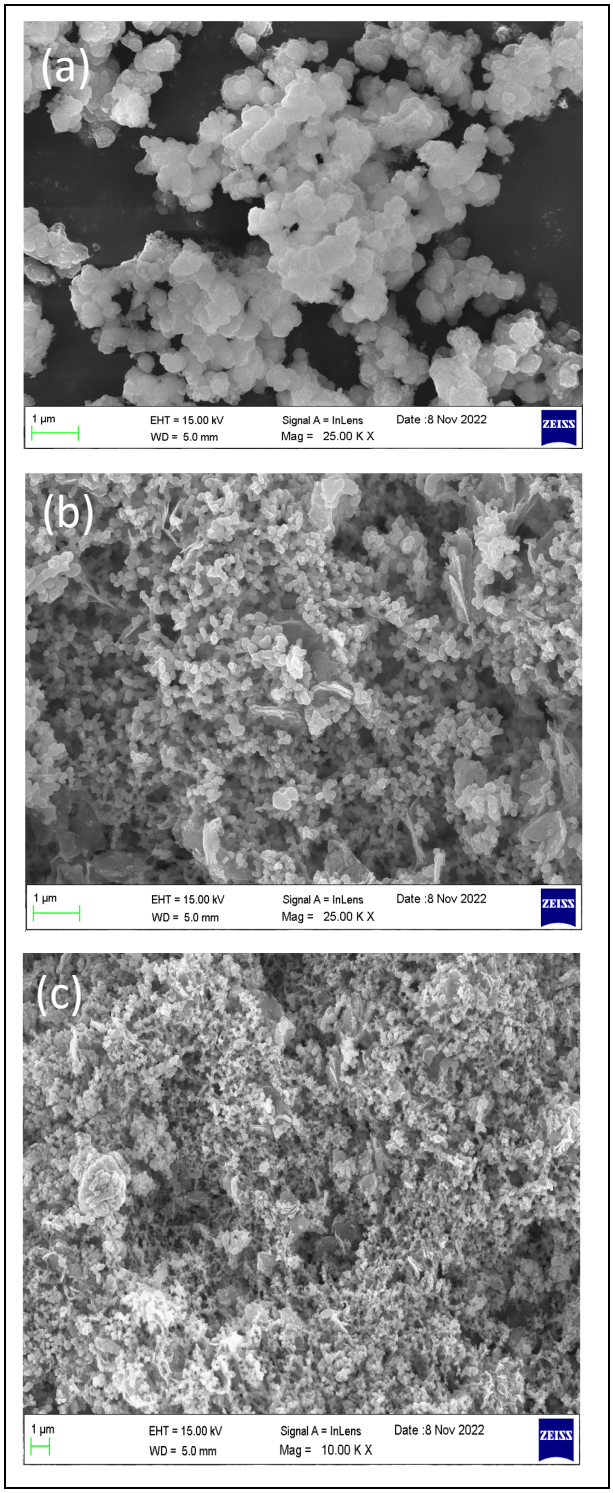


Fig. 2: FESEM images of (a) pure ZnS, (b) 2.5 M% Ni-doped ZnS nanoparticles, (c) 5.0 M% Ni-doped ZnS nanoparticles

Additionally, the uniform distribution of particle sizes in the Ni-doped ZnS samples can be linked to the solvothermal microwave irradiation synthesis technique employed. This method provides controlled thermal conditions that promote uniform growth and minimizes particle coalescence. The predominance of nearly spherical shapes among the nanoparticles further supports the effectiveness of this synthesis approach, as spherical geometries are typically favoured in processes where energy minimization is a factor. The combination of these factors not only elucidates the role of nickel doping in particle size reduction but also highlights the importance of synthesis techniques in achieving desirable material properties for potential applications in photocatalysis and optoelectronics (Kumar *et al*. 2019).

4.2 Elemental Analysis

Fig. 3 illustrates the Energy Dispersive X-ray Spectroscopy (EDX) results for pure ZnS nanoparticles alongside ZnS nanoparticles doped with 2.5 M% and 5.0 M% Ni. The EDX analysis confirms the presence of zinc, nickel, and sulphur in the samples, demonstrating that the incorporation of nickel does not disrupt the fundamental stoichiometry of the ZnS matrix. This is crucial, as maintaining the stoichiometric proportions ensures that the electronic and optical properties of the nanoparticles remain optimal for applications in photocatalysis and dye-sensitized solar cells. Moreover, the EDX findings reveal insights into the effectiveness of nickel doping in modulating the properties of ZnS nanoparticles. The slight increase in nickel concentration correlates with potential alterations in the band gap and charge carrier dynamics, which could enhance photocatalytic efficiency (Raza *et al*. 2024). By maintaining the stoichiometric balance between Zn and S while introducing nickel, these nanoparticles can effectively exploit the unique properties of transition metals, such as enhanced charge separation and improved light absorption, thereby broadening their applicability in advanced materials science and energy conversion technologies (Jothibas *et al*. 2018).

4.3 Optical Studies

The optical properties of Ni-doped ZnS nanoparticles were systematically investigated through UV-visible absorption spectroscopy (Fig. 4(a)). Notably, the absorption band edge was consistently observed between 270 nm and 370 nm across all samples. As the concentration of Ni dopant increased, a red shift in the absorption spectrum was noted, indicating a significant influence of the dopant on the electronic structure of the nanoparticles. This shift can be attributed to the quantum confinement effect, which becomes more pronounced with higher doping levels. The corresponding optical bandgap energies were determined from the energy plots (Fig.4(b)), revealing values of 3.54 eV, 3.52 eV, and 3.50 eV for 0 M%, 2.5 M%, and 5.0 M% Ni concentrations, respectively. These results suggest that as Ni concentration increases, the optical bandgap decreases, reflecting a higher charge carrier concentration that facilitates enhanced photon absorption.

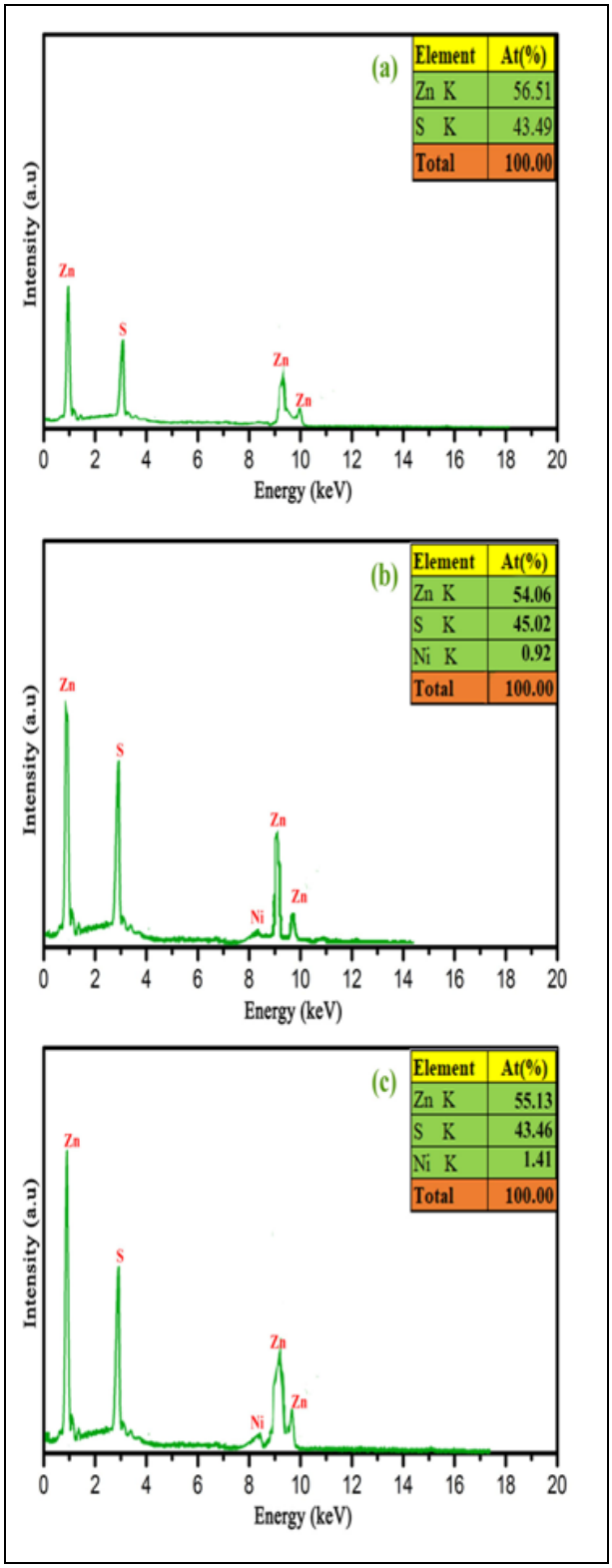


Fig. 3: EDX spectra of (a) pure ZnS, (b) 2.5 M% Ni-doped ZnS nanoparticles, (c) 5.0 M% Ni-doped ZnS nanoparticles

The decrease in the optical bandgap with increasing Ni dopant levels signifies a transition in the electronic properties of the nanoparticles, likely due to enhanced interaction between the dopant and the ZnS lattice. This increased charge carrier concentration accelerates the absorption of photons, thereby optimizing the photocatalytic potential of the Ni-doped ZnS nanoparticles. The observed modifications in optical characteristics underscore the suitability of these nanoparticles for photocatalytic applications, as they exhibit improved absorption capabilities that are essential for effective energy conversion processes (Joseph *et al*. 2022). Such findings highlight the promising nature of Ni-doped ZnS nanoparticles in various photocatalytic and optoelectronic applications, further enhancing their appeal in advanced material research (Kumar *et al*. 2019).

4.4 Photocatalytic Activity on MB Dye

The performance of photo catalysis is influenced by crystallinity, surface area, and morphology. The MB solution's peak absorbance wavelength was observed at 665 nm (Markovic *et al.* 2015). The process of photocatalysis usually commences with the absorption of photons, leading to generate electron-hole pairs. Afterwards, the charged particles spread to the surface of the sample. On the surface, they react with water, producing reactive peroxide (O_2^-) and hydroxyl radical ($^*OH^-$), which are play role for breaking down dye molecules. The process of photocatalytic activity is as follows.

$$ZnS + hv \longrightarrow e^- + h^+$$

$$e^- + O_2{}^* \longrightarrow O_2{}^-$$

$$h^+ + OH \longrightarrow {}^*OH$$

$$h^+ + H_2O \longrightarrow H^+ + {}^*OH^-$$

$$^*OH^- + \text{Methylene Blue} \longrightarrow \text{Degradation products}$$

$$^*O^- + \text{Methylene Blue} \longrightarrow \text{Degradation products}$$

The interaction of highly reactive radicals such as *OH and $*O_2^-$ with methylene blue dye is pivotal in the degradation process. These radicals initiate a series of oxidation reactions, breaking down the dye's complex structure into smaller, less harmful molecules. The effectiveness of the photocatalytic activity is quantitatively measured using the percentage of degradation (D), calculated with the formula (Pouretodal *et al*. 2010):

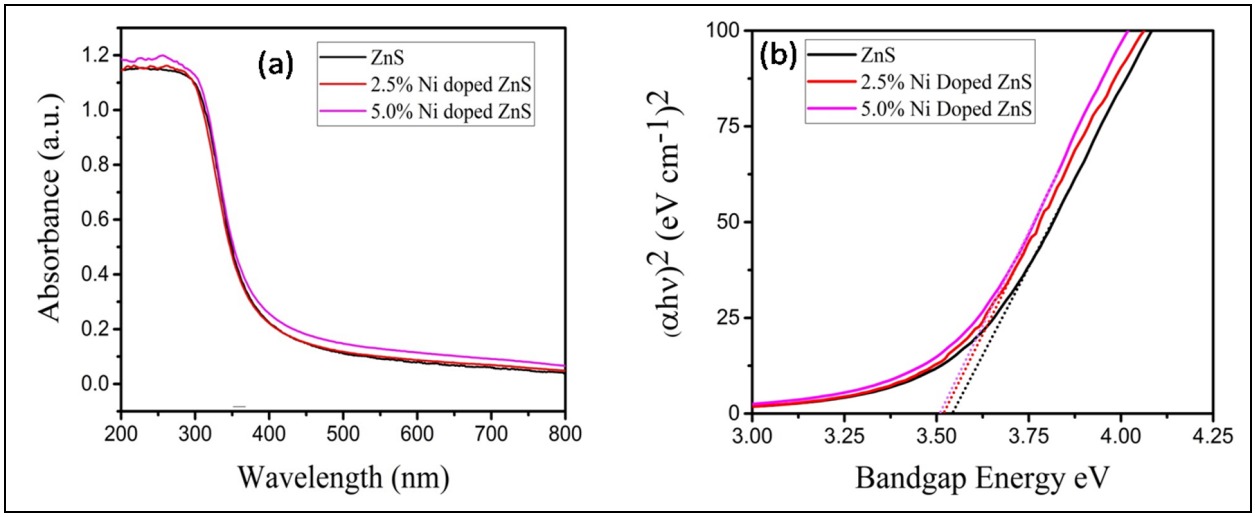


Fig.4: (a) UV-Vis spectra of Ni (0, 2.5, and 5.0) M% doped ZnS nanoparticles and (b) Tauc plot for Ni (0, 2.5, and 5.0) M% doped ZnS nanoparticles

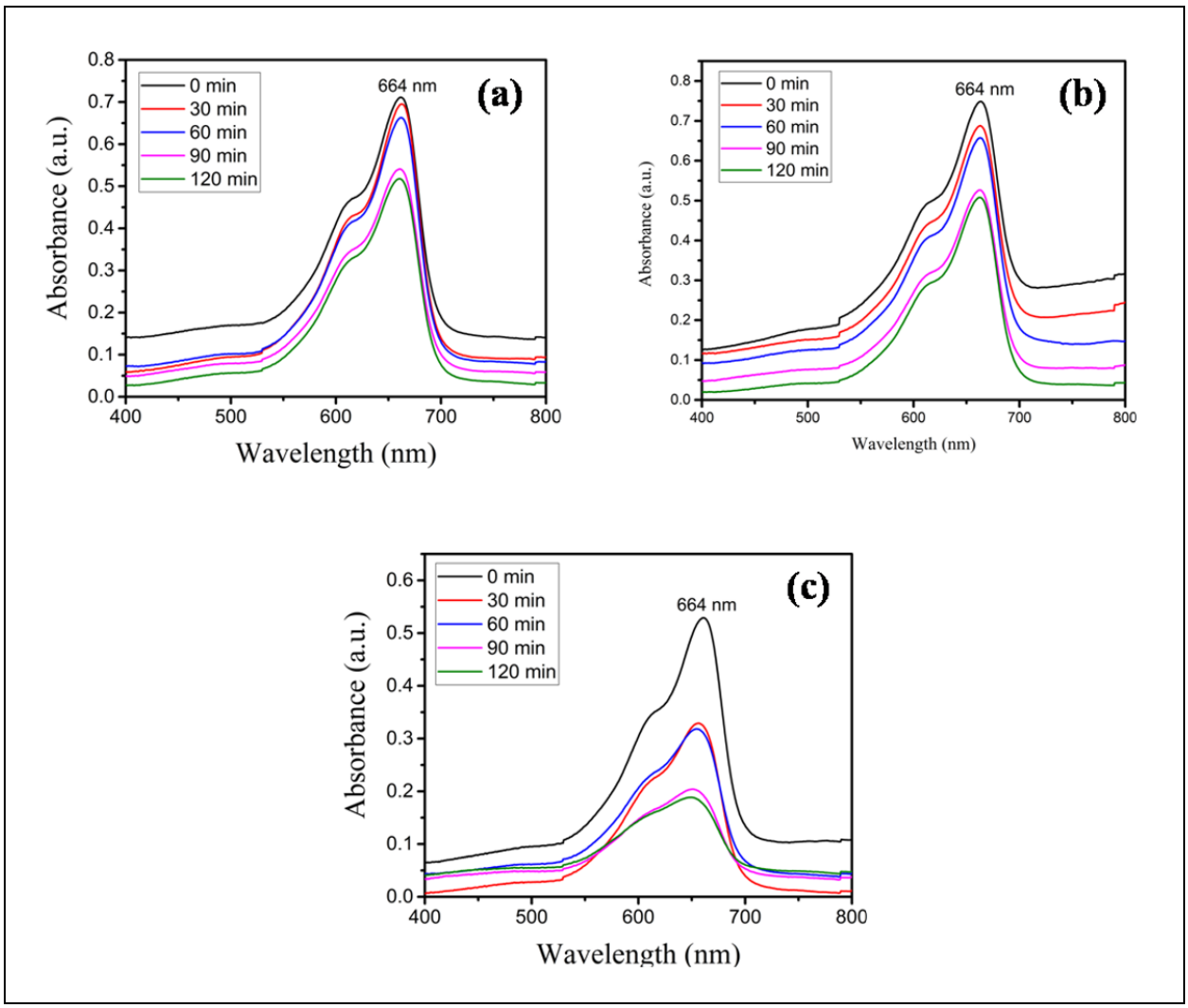


Fig. 5: Photodegradation response of MB in water under UV radiation, (a) Pure ZnS, (b) 2.5 M% Ni and (c) 5.0 M% Ni-doped ZnS nanoparticles

$$\% D = [(C_0\text{-}C)/C_0]*100 \% \quad \ldots (2),$$

where C_0 is the initial concentration of the dye and C is the concentration at various time intervals during UV irradiation, up to 120 minutes. This method allows for a clear assessment of the catalyst's efficiency in reducing dye concentration over time.

Experimental results reveal that the degradation efficiencies for pure and Ni-doped ZnS catalysts are 60.2 % for pure ZnS, 64.5% for 2.5 M% Ni-doped ZnS, and an impressive 75.2% for 5.0 M% Ni-doped ZnS nanoparticles. This data indicates a clear trend in which photocatalytic efficiency increases significantly with higher Ni doping concentration. The substantial enhancement in degradation efficiency with higher Ni doping can be attributed to several factors. Firstly, the optimal 5.0 M% Ni doping may create more active sites for the adsorption of MB dye, allowing for increased interaction with reactive radicals. Furthermore, the presence of Ni can facilitate better charge separation, reducing recombination rates of electron-hole pairs and thereby increasing the availability of these charge carriers for oxidative reactions (Jothibas *et al.* 2018). This trend underscores the importance of optimizing dopant concentration in enhancing photocatalytic performance, making these Ni-doped ZnS nanostructures particularly effective for environmental remediation applications.

5. CONCLUSION

Pure and Ni-doped ZnS nanoparticles (0, 2.5, and 5.0 mol%) were synthesized *via* SMI, enabling uniform growth and controlled particle size. XRD confirmed a cubic ZnS phase with successful Ni incorporation and no impurity peaks. Field emission scanning electron microscopy showed reduced particle size with increasing Ni content, while EDX verified the presence of Zn, Ni, and S with maintained stoichiometry.

UV–Vis analysis indicated a decrease in band gap with higher Ni doping, enhancing charge carrier dynamics. Photocatalytic performance improved significantly with increasing Ni concentration, with 5.0 mol% Ni–ZnS achieving 75.2% degradation of methylene blue. The enhancement is attributed to improved charge separation, increased reactive species generation, and higher active site availability, demonstrating the effectiveness of Ni doping in tuning ZnS for photocatalytic applications.

ACKNOWLEDGEMENT

The authors wish to extend their profound gratitude to the Avinashilingam Institute for Home Science and Higher Education for Women, Coimbatore, for their invaluable support in the characterization studies that were pivotal to this research. We would also like to express our heartfelt appreciation to Dr. P. Gowdhaman for his unwavering assistance throughout this work. Additionally, our sincere thanks go to Dr. T. Venkatesan for his insightful guidance and expertise, which significantly enriched our understanding and execution of the project. Their combined contributions have greatly enhanced the quality and depth of our study.

FUNDING

There is no funding source.

CONFLICT OF INTEREST

The authors declared no conflict of interest in this manuscript regarding publication.

COPYRIGHT

This article is an open-access article distributed under the terms and conditions of the Creative Commons Attribution (CC BY) license (http://creativecommons.org/licenses/by/4.0/).



REFRENCES:

Amiri, O., Hosseinpour, M. S. M., Rad, M. M. and Abdvali, F., Sonochemical synthesis and characterization of CdS/ZnS core–shell nanoparticles and application in removal of heavy metals from aqueous solution, *Super lattices Microstruct.*, 66, 67-75 (2014). https://doi.org/10.1016/j.spmi.2013.11.003

Chen, J., Xin, F., Qin, S. and Yin, X., Photocatalytically reducing CO2 to methyl formate in methanol over ZnS and Ni-doped ZnS photocatalysts, *Chem. Eng. J.*, 230, 506-512 (2013). https://doi.org/10.1016/j.cej.2013.06.119

Farooqi, M. M. H. and Srivastava, R. K., Structural, optical and photoconductivity study of ZnS nanoparticles synthesized by a low temperature solid state reaction method, *Mater. Sci. Semicond. Process*., 20, 61-67 (2014). https://doi.org/10.1016/j.mssp.2013.12.028

Gowdhaman, P., Praveen, V. N., Saravanan, R. S. S., Venkateswari, P. and Pandya, H. M., Facile synthesis of undoped and Sn doped CdS nanoparticles for dye-sensitized solar cell applications, *Opt. Mater*., 120, 111465 (2021). https://doi.org/10.1016/j.optmat.2021.111465

Hussein, H. M.. Structural and optomagnetic properties of Ni-doped ZnS synthesized by solvothermal method, *Colloid J.,* 85(4), 666-672 (2023). https://doi.org/10.1134/S1061933X22600610

Joseph, A., Billakanti, S., Pandit, M. A., Khatun, S., Rengan, A. K. and Muralidharan, K., Impact of bandgap tuning on ZnS for degradation of environmental pollutants and disinfection, *Environ. Sci. Pollut. Res.,* 29(37), 56863-56875(2022). https://doi.org/10.1007/s11356-022-19677-y

Jothibas, M., Manoharan, C., Jeyakumar, S. J., Praveen, P., Punithavathy, I. K. and Richard, J. P., Synthesis and enhanced photocatalytic property of Ni-doped ZnS nanoparticles, *Sol. Energy*, 159, 434-443 (2018). https://doi.org/10.1016/j.solener.2017.10.055.

Kaur, Jagdeep, Manoj Sharma, and Pandey, O. P., Photoluminescence and photocatalytic studies of metal ions (Mn and Ni) doped ZnS nanoparticles, *Opt. Mater*., 47, 7-17 (2015). https://doi.org/10.1016/j.optmat.2015.06.022

Krishnan, B., Shaji, S., Acosta, E. M. C., Acosta, E. E. B., Castillo-Ortega, R., Zayas, M. E. and Cortese, B., Group II–VI Semiconductors, *Semiconduct. Syn. Prop. Appl.*, 397-464 (2019). https://doi.org/10.1007/978-3-030-02171-9_7

Kumar, S. and Verma, N. K., Effect of Ni-doping on optical and magnetic properties of solvothermally synthesized ZnS wurtzite nanorods, *J. Mater. Sci.: Mater. Electron* ., 25, 785-790 (2014). https://doi.org/10.1007/s10854-013-1646-8

Kumar, V., Rawal, I., Kumar, V. and Goyal, P. K., Efficient UV photodetectors based on Ni-doped ZnS nanoparticles prepared by facial chemical reduction method, *Physica B: Condensed Matter.,* 575, 411690(2019). https://doi.org/10.1016/j.physb.2019.411690

Marković, S., Stanković, A., Lopičić, Z., Lazarević, S., Stojanović, M. and Uskoković, D., Application of raw peach shell particles for removal of methylene blue, *J. Environ. Chem. Eng.*, 3(2), 716-724(2015). https://doi.org/10.1016/j.jece.2015.04.002

La, P. F. A., Ferrer, M. M., De, S., Y. V., Raubach, C. W., Longo, V. M., Sambrano, J. R. and Varela, J. A., Synthesis of wurtzite ZnS nanoparticles using the microwave assisted solvothermal method, *J. Alloys Compd*., 556, 153-159 (2013). https://doi.org/10.1016/j.jallcom.2012.12.081

Patel, P. C., Ghosh, S. and Srivastava, P. C., Bound magnetic polaron driven room-temperature ferromagnetism in Ni-doped ZnS nanoparticles, *Mater. Chem. Phy*., 216, 285-293 (2018). https://doi.org/10.1016/j.matchemphys.2018.05.065

Pouretedal, H. R. and Keshavarz, M. H., Synthesis and characterization of Zn1− XCuXS and Zn1− XNiXS nanoparticles and their applications as photocatalyst in Congo red degradation, *J. Alloys Compd.*, 501(1), 130-135 (2010). https://doi.org/10.1016/j.jallcom.2010.04.058

Rajabi, H. R. and Farsi, M., Effect of transition metal ion doping on the photocatalytic activity of ZnS quantum dots: synthesis, characterization, and application for dye decolorization*, J. Mol. Catal. A: Chem*., 399, 53-61 (2015). https://doi.org/10.1016/j.molcata.2015.01.029

Ramasamy, V., Praba, K., Murugadoss, G., Synthesis and study of optical properties of transition metals doped ZnS nanoparticles, *Spectrochim. Acta, Part A*, 96, 963-971 (2012). https://doi.org/10.1016/j.saa.2012.07.125.

Raza, M., Farooq, U., Khan, S. A., Ullah, Z., Khan, M. E., Ali, S. K. and Zakri, W., Preparation and Spectrochemical characterization of Ni-doped ZnS nanocomposite for effective removal of emerging contaminants and hydrogen Production: Reaction Kinetics, mechanistic insights, *Spectro. Acta Part A: Mol. Biomol. Spectros.,* 124513 (2024). https://doi.org/10.1016/j.saa.2024.124513

Saravanan, R. S. S. and Mahadevan, C. K., Photoluminescence and electrical impedance measurements on alloyed Zn (1− x) CdxS nanocrystals, *J. Alloys Compd.*, 541, 115-124 (2012). https://doi.org/10.1016/j.jallcom.2012.06.048

Srivastava, R. K., Pandey, N. and Mishra, S. K., Effect of Cu concentration on the photoconductivity properties of ZnS nanoparticles synthesized by co-precipitation method, *Mater. Sci. Semicond. Process*., 16(6), 1659-1664 (2013). https://doi.org/10.1016/j.mssp.2013.06.009

Suganthi, N. and Pushpanathan, K., Photocatalytic degradation and antimicrobial activity of transition metal doped mesoporous ZnS nanoparticles, *Int. J. Environ. Sci. Technol.*, 16, 3375-3388 (2019). https://doi.org/10.1007/s13762-018-1811-y

Tiwary, K. P., Ali, F., Choubey, S. K., Mishra, R. K. and Sharma, K., Doping effect of Ni2+ ion on structural, morphological and optical properties of Zinc sulfide nanoparticles synthesized by microwave assisted method, *Optik*, 227, 166045 (2021). https://doi.org/10.1016/j.ijleo.2020.166045

Wang, X., Peng, D., Huang, B., Pan, C. and Wang, Z. L., Piezophotonic effect based on mechanoluminescent materials for advanced flexible optoelectronic applications, *Nano Energy*, 55, 389-400 (2019). https://doi.org/10.1016/j.nanoen.2018.11.014

Wu, M., Wei, Z., Zhao, W., Wang, X. and Jiang, J., Optical and magnetic properties of Ni-doped ZnS diluted magnetic semiconductors synthesized by hydrothermal method, *J. Nanomaterials*., 2017(1), 1603450 (2017). https://doi.org/10.1155/2017/1603450

Xu, X., Li, S., Chen, J., Cai, S., Long, Z. and Fang, X., Design principles and material engineering of ZnS for optoelectronic devices and catalysis, *Adv. Funct. Mater*., 28(36), 1802029 (2018). https://doi.org/10.1002/adfm.201802029

Zein, R. and Alghoraibi, I., Influence of bath temperature and deposition time on topographical and optical properties of nanoparticles ZnS thin films synthesized by a chemical bath deposition method, *J. Nanomater.*, 2019(1), 7541863 (2019). https://doi.org/10.1155/2019/7541863